Applied Radiation and Isotopes 132 (2018) 129–134

Contents lists available at ScienceDirect

Applied Radiation and Isotopes

journal homepage: www.elsevier.com/locate/apradiso

Monte Carlo calculations of electrons impinging on a copper target: A comparison of EGSnrc, Geant4 and MCNP5

John Paul Archambault

National Research Council Canada, 1200 Montreal Road, Ottawa ON, Canada K1A 0R6

ARTICLE INFO

Keywords:
Monte Carlo
Electrons
Bremsstrahlung
Copper target

ABSTRACT

A simple geometry is used to compare several of the available Monte Carlo software codes for radiation transport. EGSnrc, Geant4 and MCNP5 are all used to calculate the photon fluence produced from electrons incident on a copper target. Four energies for the isotropic point source are chosen to simulate the average and maximum emission energies of ^{32}P and ^{90}Y: (0.7, 1.71) MeV and (0.93, 2.28) MeV, respectively. The energy deposition in the copper target, the electron current at the target and the computational efficiency are also calculated. EGSnrc is found to be the only self-consistent code when comparing results calculated using the default transport parameters of the condensed history mode with those calculated in the single scattering mode.

1. Introduction

The Monte Carlo (MC) method for solving problems involving radiation transport is a valuable tool, used in many aspects of research, from aiding in the design of radiation detectors, to understanding particle interactions with materials in and around such detectors. This is true in radionuclide metrology, for example, where various MC software codes have been used to calculate the calibration coefficients of both γ- and β-emitting radionuclides (de Vismes and Amiot, 2003; Laedermann et al., 2004; Thiam et al., 2016; Amiot et al., 2012; Bobin et al., 2017). The calibration of radionuclide calibrators for γ-emitting radionuclides is very well understood (Michotte et al., 2006). However, the detection of pure β-emitting radionuclide sources is more indirect, as many of the β-particles are absorbed in the source solution itself or interact with the inactive components of the detector, producing bremsstrahlung radiation. It is essential, then, that the interactions of β-radiation be properly described in the MC codes if they are to be used in the study of radiation detectors.

The simulation of β-radiation is complicated due to the large number of interactions which an electron undergoes during its transport through a medium. In most real-life examples, an analogue simulation of the motion is prohibitively inefficient. To overcome these inefficiencies, Berger (1963) developed the condensed history (CH) method of calculating electron transport, which determines the cumulative effect of multiple electron steps into one larger step. The approximation accounts for the particle's energy change as well as the change in the particle's direction and position. This approximation is often referred to as multiple scattering and the changes in energy, direction and position are calculated by sampling various multiple scattering distributions. A thorough review of many of the current CH implementations can be found in Kawrakow and Bielajew (1998).

This study compares several of the available Monte Carlo software codes in the calculation of the photon fluence produced from electrons incident on a copper target. EGSnrc (Kawrakow et al., 2013), Geant4 (Agostinelli et al., 2003) and MCNP5 (X-5 Monte Carlo Team, 2003) all calculate electron and photon transport in specified media using Monte Carlo techniques and have been chosen for this study. While this study is a response to a discussion held at an International Committee for Radionuclide Metrology (ICRM) Working Group meeting about a possible comparison between different MC codes (R. Galea 2014, personal communication), it also has applicability in many areas of radiation physics (Faddegon et al., 2008; Pandola et al., 2015). The results found for the simple geometry chosen for study here can provide a baseline which can be used when more complex experimental setups, such as complete radionuclide calibrator systems, are tested.

The success of MC codes in describing experimental data depends on many factors, including the algorithms for calculating radiation transport, the descriptions of geometries used in the simulations and ultimately on the particle cross sections used in the calculations (Bochud et al., 2015). Using a simple setup reduces questions on geometry differences as well as possibilities for areas where the user codes can differ.

In Section 2, the details of the Monte Carlo study are given. The particle source, the geometry and the materials are provided. The results and analysis of the study are provided in Section 3. Finally, the conclusions are given in Section 4.

E-mail address: JohnPaul.Archambault@nrc-cnrc.gc.ca.

https://doi.org/10.1016/j.apradiso.2017.11.023
Received 15 June 2017; Received in revised form 29 September 2017; Accepted 15 November 2017
Available online 27 November 2017
0969-8043/ Crown Copyright © 2017 Published by Elsevier Ltd. All rights reserved.

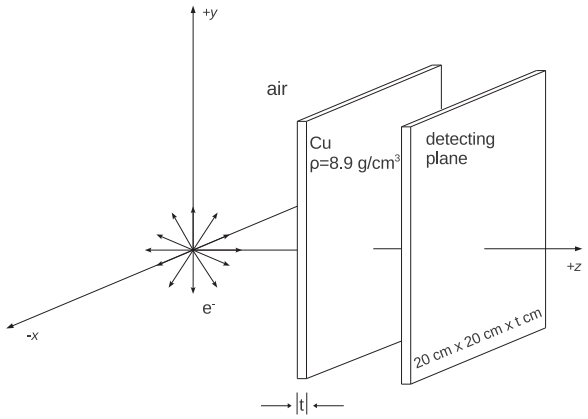

Fig. 1. Schematic diagram of the metallic target geometry.

2. Monte Carlo details

EGSnrc version V4-r2-4-0, Geant4 version 9.6 (with patch 02) and MCNP5 version 1.60 are used to study the geometry illustrated in Fig. 1. An isotropic, mono-energetic electron point source is positioned at the origin with a copper target of dimension $20 \times 20 \times t$ cm^3 placed at distance $z = 1$ cm away. The bremsstrahlung photons created in the target are detected using a detecting plane placed 1 cm away from the copper target. The detector is given the same dimensions as the copper target and four energies for the point source are chosen to simulate the average and maximum emission energies of phosphorus-32 (^{32}P) and yttrium-90 (^{90}Y): (0.7, 1.71) MeV and (0.93, 2.28) MeV, respectively. The thickness of the copper target is varied to represent the continuous slowing down approximation (CSDA) range of the specified material at the corresponding energy. A summary of the details of the simulation geometry is provided in Table 1.

The ultimate goal of the study is to calculate the photon energy fluence at the detecting plane, however several additional quantities are calculated and compared between the codes: the energy deposition in the copper target, the electron current at the copper target and finally the integrated photon fluence on the surface of the detector. For surface calculations, the surface is defined as the plane facing the source, unless otherwise specified. The current calculations at the front face of the copper target count the number of particles crossing the surface and are categorized as forward and backward current depending on the sign of the z-component of the electron's direction as it passes the surface. The forward current corresponds to a $(+)z$-direction while the backward current corresponds to the $(-)z$-direction.

An EGS++ application was written to calculate the energy deposited in the copper target, the surface currents and fluences. In Geant4, the energy deposited in the copper target is calculated using the `G4PSEnergyDeposit` primitive scorer, while the surface currents are calculated using `G4PSFlatSurfaceCurrent` and the fluence calculated using `G4PSFlatSurfaceFlux`. Finally, in MCNP5, the surface currents are calculated using `tally 1`, the surface fluences calculated using `tally 2` and the energy deposition calculated using `tally 8*`.

Table 1
Summary of details used in the geometry of the Monte Carlo simulations.

Isotope	Energy [MeV]	CSDA Range [g/cm^2]	Thickness [cm]
^{32}P	0.7	0.40	0.05
	1.71	1.20	0.13
^{90}Y	0.93	0.56	0.06
	2.28	1.60	0.18

Table 2
Summary of the default condensed history algorithms and methods for evaluation of bremsstrahlungcross sections used by each of the MC codes for the particle energies studied.

MC Code	Condensed history	Bremsstrahlung cross sections
EGSnrc	PRESTA-II (Kawrakow and Bielajew, 1998)	Koch and Motz (1959)
Geant4	Urban (2006), Lewis (1950)	Seltzer and Berger (1986)
MCNP5	Goudsmit and Saunderson (1940), Landau (1944), Blunck and Leisegang (1950)	Seltzer (1988), Seltzer and Berger (1985), Seltzer and Berger (1986)

The determination of the surface fluence requires the calculation of the cosine of the angle between the particle direction and the surface in question, denoted by μ. In the case where a particle is traveling parallel to the surface, the cosine is zero and the calculation of the fluence diverges. Most software employ a prescription which limits the value of the cosine once a certain threshold is reached. For example, if the cosine is less than 0.1, MCNP5 sets the value to $\mu = 0.05$. For purposes of the comparison, this prescription is used for each of the codes.

Because of the simple geometry, the single scattering implementations of EGSnrc and Geant4 could be run with reasonable computing times. This is accomplished by using a large value (e.g. 100) for the skin depth parameter in EGSnrc and by using the `G4StandardSS` physics list in Geant4. No such mode is available in MCNP5, so MCNP5 is compared to EGSnrc throughout the study. In addition to the single scattering calculations, the condensed history (CH) modes are used for each of the codes. For EGSnrc, a skin depth value of 3 is used, while for Geant4 the `G4StandardEM` physics list is used and unless otherwise stated all the default transport parameters are used. A summary of the default CH algorithms and methods for cross section evaluation for the particle energies studied here used in each of the codes is provided in Table 2. More detailed information about each can be found in the respective manuals.

In both EGSnrc and MCNP5, the electron and photon energy cut-off values are set to 1 keV, while the default cut-off values are used in Geant4. Where appropriate, different physics lists are tested in Geant4 and non-default parameters of MCNP5 are studied and are discussed. Throughout the report single scattering results are represented by closed symbols and all CH results are represented as open symbols. Unless otherwise indicated, the results have a statistical uncertainty of approximately 0.1% for all quantities of interest and are quoted as $k = 1$.

3. Results

3.1. Energy deposition

The energy deposited in the copper target for each of the incident energies is presented in Fig. 2. The absolute energy deposition is provided in Fig. 2a, calculated using the single scattering mode of EGSnrc. For purposes of clarity, the Geant4 results are presented as the ratio (R) to the EGSnrc results. Differences in the results are under 1% for each of the source and target scenarios with the Geant4 results systematically higher than that of EGSnrc.

The results of the default condensed history calculations for each of the codes are provided in Fig. 2b, where they are presented as the ratio to their respective single scattering results. EGSnrc is consistent with its own single scattering implementation whereas the Geant4 standard physics list is systematically high with a difference reaching as much as 2%. Results are similar when the Geant4 low-energy physics lists `G4Livermore` and `G4Penelope` are used. Changing the values of `dRoverRange` and `finalRange` of the `G4EmProcessOptions` class to 0.01 and 100 nm (Poon et al., 2005), respectively, the two highest energy scenarios agree with the EGSnrc results, however the two lowest

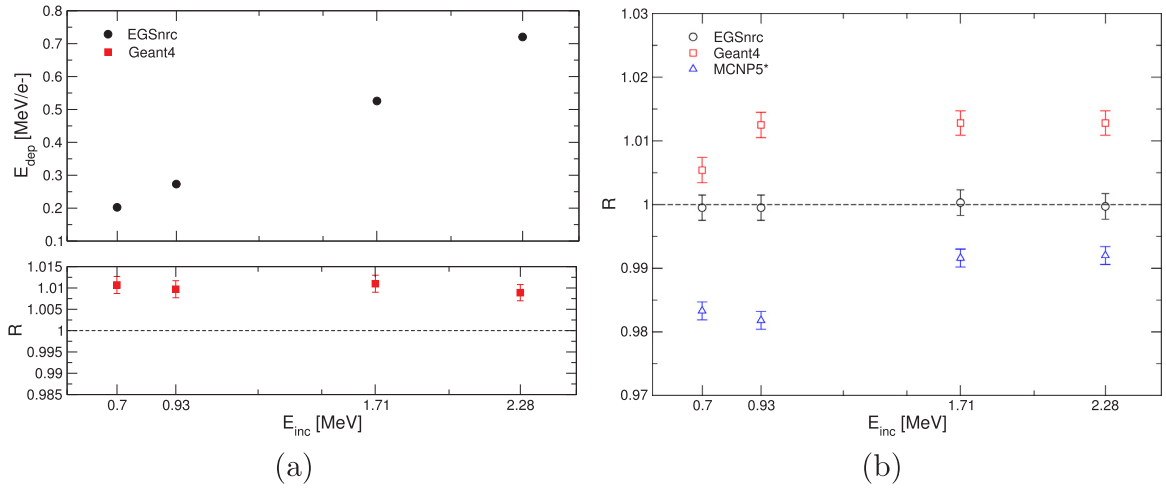

Fig. 2. Energy deposition in the copper target. (a) Single scattering calculations. The top view contains the absolute values while the bottom view contains the ratio (R) of Geant4 to EGSnrc results. (b) Condensed history results, where R is the ratio to the respective single scattering mode results (* MCNP5 is compared to EGSnrc).

energy scenario results are lower than EGSnrc at the 1% level.

MCNP5 is systematically low compared to EGSnrc, with a 2.0% difference. Changing the value of `ESTEP` on the material card for air to 10 from the default value of 3 aligns the results with those of EGSnrc for the two lowest energy scenarios, but does not affect the two highest energy scenarios. The change, however, increases the computation time by a factor of approximately 2.

As air is known to affect the simulation of electron transport in certain situations (Archambault and Mainegra-Hing, 2015), a study was completed with the air surrounding the targets switched to vacuum. This did not effect the results of the Geant4 calculations, but reduced the MCNP5 differences to 0.5% within those of EGSnrc.

3.2. Electron current

The electron current at the front face of the copper target for each of the scenarios is provided in Figs. 3 and 4. Figs. 3a and 4a give the absolute results calculated using the single scattering modes for the forward and backward current, respectively. The forward current is a measure of the number of electrons reaching the copper target directly from the source (or via scattering in the air) and should tend toward a value of 0.5 e^{-1} for an isotropic source and an infinite detection plane. For the 20 × 20 cm^2 plane, the differences in the calculated forward current between the EGSnrc and Geant4 single scattering modes are less than 0.6%, with an absolute value between 0.4625 e^{-1} and 0.475 e^{-1}, although the Geant4 results are systematically lower than those of EGSnrc. The backward current, a measure of the backscatter from the copper target, shows differences on the order of 2% for the lowest energy scenarios, but reaches approximately 10% for the highest energy scenario.

A separate study investigating the energy spectra of the backscattered electrons, calculated in single scattering mode, shows that the major differences between the EGSnrc and Geant4 results occur in the lowest and highest energy bins. A systematic study of the EGSnrc parameters demonstrates that only the parameter which controls spin effects affected the results of the backscattering. Turning the spin effects off increases the backscatter by approximately 2%.

The condensed history results are provided in Fig. 3b and Fig. 4b for the forward and backward currents, respectively. EGSnrc is within the statistical uncertainties of its own single scattering results for the forward current. Geant4 is systematically high compared to its single scattering mode, by as much as 4%. Finally, MCNP5 is systematically lower than EGSnrc with at most a 3% difference, decreasing to under 1% for the two highest energy scenarios.

For the backward current, EGSnrc is within the statistical uncertainties of its own single scattering results. Geant4 is higher than its single scattering calculation by approximately 7% for all scenarios. Changing the parameters `dRoverRange` to 0.01 reduces these

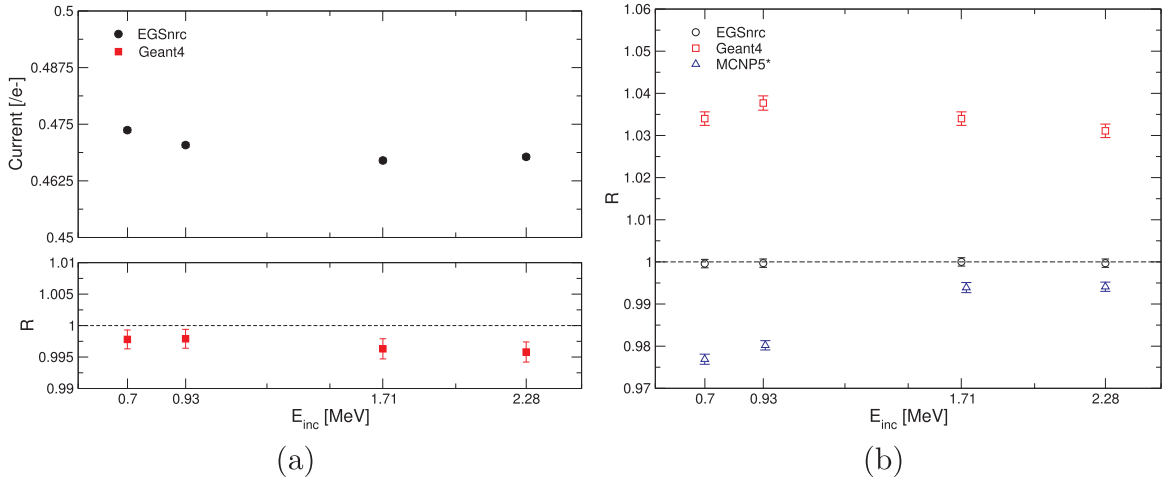

Fig. 3. Forward electron current at copper target. (a) Single scattering calculations. The top view contains the absolute values while the bottom view contains the ratio (R) of Geant4 to EGSnrc results. (b) Condensed history results, where R is the ratio to the respective single scattering mode results (* MCNP5 is compared to EGSnrc).

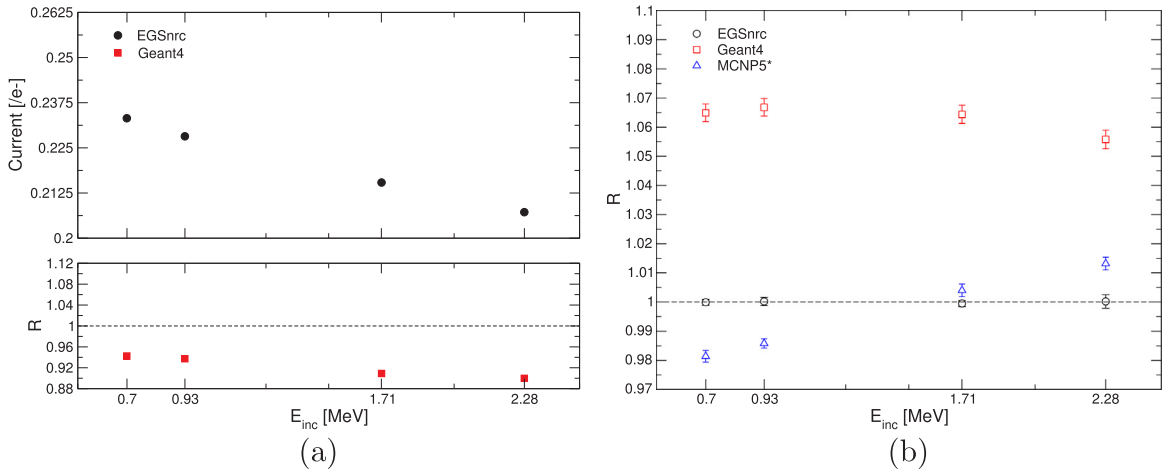

Fig. 4. Backward electron current at copper target. (a) Single scattering calculations. The top view contains the absolute values while the bottom view contains the ratio (R) of Geant4 to EGSnrc results. (b) Condensed history results, where R is the ratio to the respective single scattering mode results (* MCNP5 is compared to EGSnrc).

differences to the range of 2–4%, with the computing time increasing by a factor of about 6. MCNP5 is lower than EGSnrc by approximately 2% for the lowest energy scenario but higher by 1% for the highest energy scenario. For more in-depth studies of backscatter calculations, see Ali and Rogers (2008b), Ali and Rogers (2008a), Kim et al. (2015), Basaglia et al. (2015).

3.3. Photon fluence

The integrated photon fluence at the front plane of the detector is provided in Fig. 5 for the single scattering modes (5a) and condensed history modes (5b). The EGSnrc and Geant4 single scattering results are within 1% of each other. The EGSnrc condensed history results are consistent with the single scattering mode calculations, while the Geant4 CH results are up to 2% lower than its single scattering results. The MCNP5 results are systematically high, with differences of approximately 5–10% from the single scattering mode results of EGSnrc.

A calculation of the number of photons leaving the back surface of the copper target shows the same size of differences between EGSnrc and MCNP5 at this level in the simulation, suggesting that there are differences in the generation of bremsstrahlung photons in the two codes. MCNP5 has three algorithms available to calculate the energy at which to sample the cross sections (X-5 Monte Carlo Team, 2003): (1) the default MCNP algorithm, (2) the integrated tiger series (ITS) algorithm and (3) the energy- and step-specific (ESS) algorithm. The different algorithms are chosen for the simulation using the DBCN card. When the simulations are run with each of the different algorithms, both the ITS and the energy-specific algorithms calculate a reduced photon fluence at the detector plane to within 1–2% of the EGSnrc results for all four scenarios. This reduction in the photon fluence, however, comes with a reduction in the number of backscattered electrons at the front face of the copper target on the order of 4–6% for all scenarios investigated.

The photon energy fluence results are given in Fig. 6. Fig. 6a illustrates the absolute energy spectrum as calculated in the single scattering mode of EGSnrc, where the lines are included only to guide the eye. In order to reduce uncertainties in regions of low photon sampling, the variance reduction technique of radiation splitting was employed, using a splitting number of 10. All four scenarios have peak photon energies at approximately 250 keV, with a rapid decrease in the fluence as a function of energy. Also shown are the Geant4 single scattering results. In general, the results agree with EGSnrc within 5%, however larger differences can be seen in the low and high energy bins.

Fig. 6b provides the comparison of the condensed history methods for each code to that of single scattering for the calculation of the photon energy fluence. For reasons of clarity, only the scenario for the 0.7 MeV electron source is shown, although similar results were found for each of the other scenarios. The EGSnrc CH results agree within statistical uncertainties. The MCNP5 results were calculated using the energy- and step-specific algorithm and radiation splitting was also

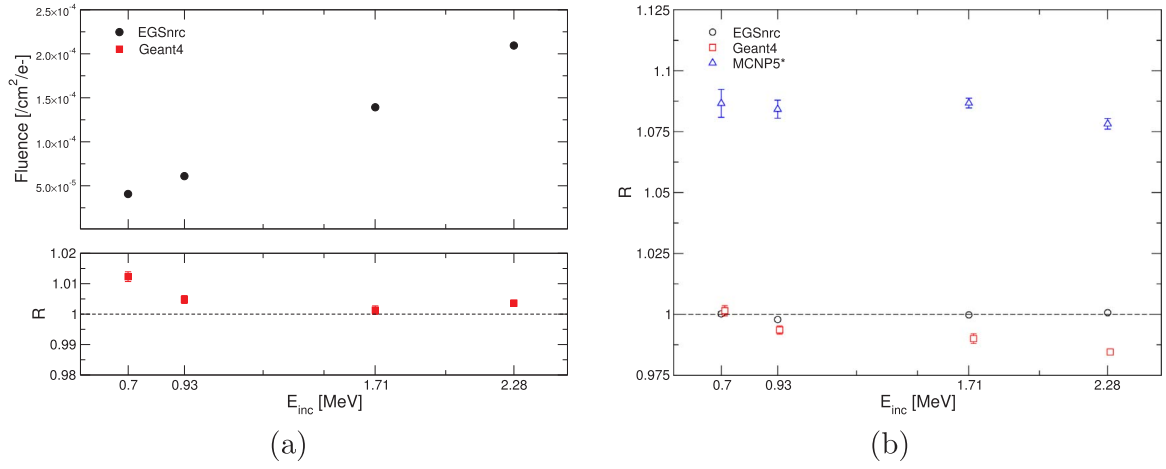

Fig. 5. Total photon fluence at the detector. (a) Single scattering calculations. The top view contains the absolute values while the bottom view contains the ratio (R) of Geant4 to EGSnrc results. (b) Condensed history results, where R is the ratio to the respective single scattering mode results (* MCNP5 is compared to EGSnrc).

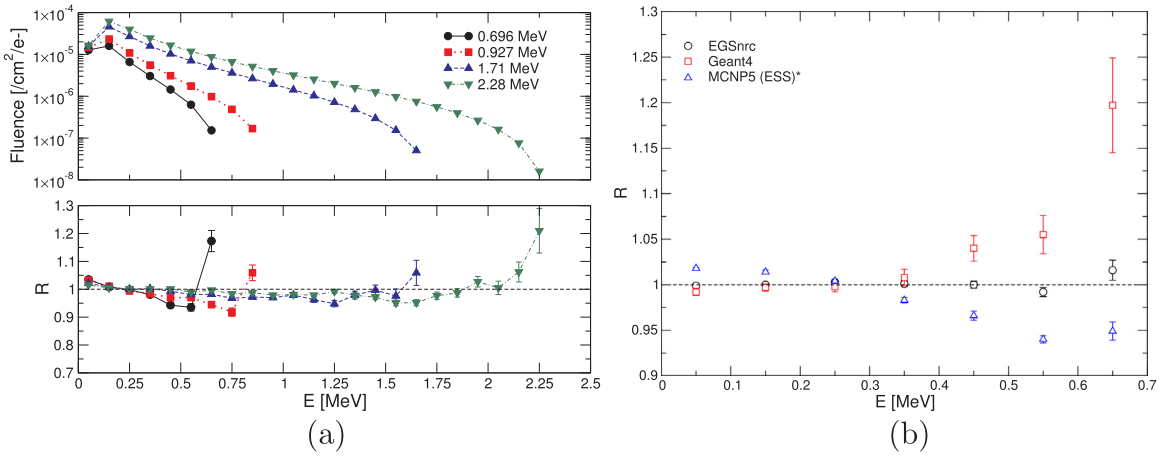

Fig. 6. Photon energy fluence at the detector. (a) Single scattering calculations. The top view contains the absolute values while the bottom view contains the ratio (R) of Geant4 to EGSnrc results. (b) Condensed history results for the 0.7 MeV scenario, where R is the ratio to the respective single scattering mode results (* MCNP5 is compared to EGSnrc).

employed in MCNP5 using the `BBREM` card. MCNP5 is within 5% of EGSnrc for all energies. Geant4 differs from its own single scattering results as much as 5% for all but the last energy bin, where the difference reaches the 20% level.

3.4. Computational efficiency

An important aspect of Monte Carlo simulations is the time required to reach a result with a certain statistical uncertainty. A measure of this is known as the computational efficiency and is defined as

$$\epsilon = \frac{1}{\sigma^2 T}, \tag{1}$$

where σ is the standard deviation of the result in question and T is the CPU time required for the calculations, measured in seconds. A smaller statistical uncertainty and shorter computation time leads to a higher computational efficiency.

The computational efficiencies for the copper target system are provided in Fig. 7 for both the single scattering and condensed history calculations. The efficiencies are calculated with respect to the uncertainty on the calculation of the energy deposited in the target. Variance reduction techniques are not considered and the lines connecting the data are provided only for clarity. Fig. 7a compares the computational efficiencies single scattering calculations with the CH calculations with the default parameters of each of the codes. As expected, the single scattering modes are less efficient than their corresponding condensed history modes. However the EGSnrc single scattering mode is as efficient as the MCNP5 calculations and a factor of approximately 10 more efficient than the Geant4 single scattering mode. The Geant4 condensed history mode is the most efficient for the three highest energy scenarios, with the efficiency increasing as the energy of the incident electron increasing.

Fig. 7 provides the same computational efficiencies calculated for the condensed history modes with the altered parameters (eg. `G4EmProcessOptions` in Geant4 and `ESTEP` and energy straggling algorithm in MCNP5). Both Geant4 and MCNP5 condensed history efficiencies drop below that of the EGSnrc single scattering efficiencies, with Geant4 dropping to the level of its own single scattering mode.

4. Conclusions

Three Monte Carlo software packages are used to study the bremsstrahlung photon energy fluence produced via an isotropic point source of electrons impinging a copper target. The monoenergetic electron energies are chosen as the mean and maximum energies of ^{32}P and ^{90}Y while the target thickness is chosen to correspond to the electron range, calculated using the CSDA approximation for the corresponding electron energy. The energy deposited in the copper target, the electron current at the front face of the target and the photon fluence behind the target are calculated using EGSnrc, Geant4 and MCNP5. Because of the simple geometry under study, the single scattering modes of EGSnrc and Geant4 are run in reasonable times, are compared and are used as references for the condensed history methods. No such mode is available in MCNP5, so the results of the MCNP5 calculations are

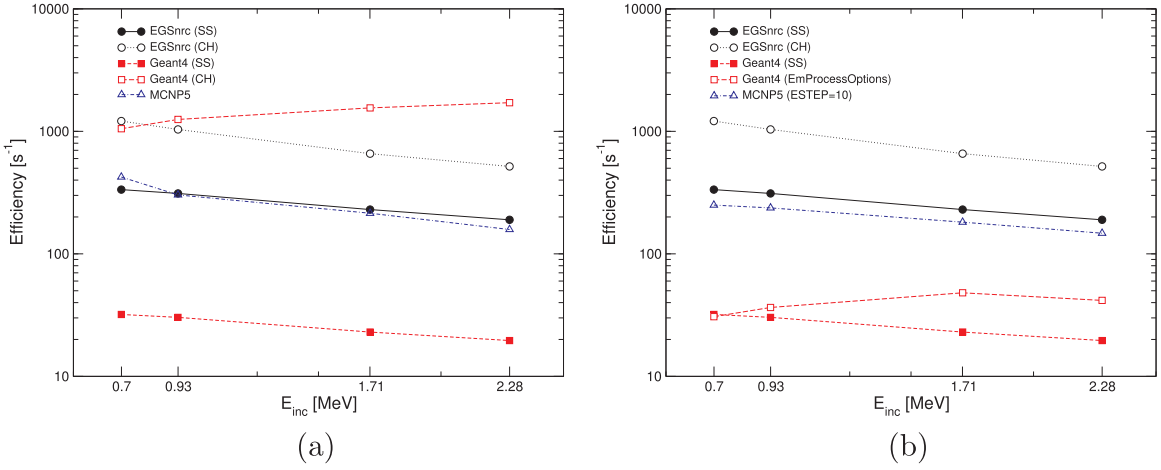

Fig. 7. Computational efficiencies, with respect to the uncertainty of the energy deposition in the copper target. (a) Default parameters and (b) altered parameters.

compared with EGSnrc single scattering throughout.

The single scattering mode calculations of the energy deposited in the copper target with EGSnrc and Geant4 are within 1% of each other, with Geant4 lying systematically higher. The differences in the forward electron current at the copper target are less than 0.5% while the differences in the backward current at the copper target increase up to a maximum difference of 8%. The two codes differ by up to 2% in calculating the integrated photon fluence at the detector.

The condensed history mode of EGSnrc is consistent, within statistical uncertainties of 0.1%, with its single scattering mode for all quantities of interest. It is the only code studied here which is self-consistent with respect to its single scattering and condensed history modes when using the default transport parameters.

The condensed history mode of Geant4 differs from its single scattering results for calculations of the energy deposition by 1–2% while the forward calculations differed by 3–4%. The backward electron backscatter was found to differ by 6–8%. Finally, the differences in the integrated photon fluence were less than 2%.

MCNP5 is systematically lower than EGSnrc in the calculation of energy deposition in the copper target, differing up to 2%. Both the forward and backward current also differ up to 3%. The integrated photon fluence at the detector is found to be systematically higher by about 10%. Changing the energy-straggling algorithm from the default to either the integrated tiger series algorithm or the energy- and step-specific algorithm reduces this difference to about 1–2%, but comes with a corresponding drop in the backward current of 4–6%.

Using the default transport parameters, the Geant4 condensed history mode has the highest computational efficiency, however changing the parameters to obtain consistency with its single scattering mode reduces the efficiency to that comparable with the single scattering mode. Of the codes considered, EGSnrc has the highest computational efficiency when self-consistency between the single scattering and condensed history modes is considered.

Acknowledgments

The author would like to thank Raphael Galea of the National Research Council Canada for helpful discussions regarding the study.

References

Agostinelli, S., Allison, J., Amako, K., Apostolakis, J., Araujo, H., Arce, P., Asai, M., Axen, D., Banerjee, S., Barrand, G., et al., 2003. GEANT4 - a simulation toolkit. Nucl. Inst. Methods A 506, 250–303.

Ali, E., Rogers, D., 2008a. Benchmarking EGSnrc in the kilovoltage energy range against experimental measurements of charged particle backscatter coefficients. Phys. Med. Biol. 53 (6), 1527–1544.

Ali, E.S.M., Rogers, D.W.O., 2008b. Energy spectra and angular distributions of charged particles backscattered from solid targets. J. Phys. D: Appl. Phys. 41 (5), 055505.

Amiot, M., Mesradi, M., Chist, V., Morin, M., Rigoulay, F., 2012. Comparison of experimental and calculated calibration coefficients for a high sensitivity ionization chamber. Applied Radiation and Isotopes 70 (9), 2232 – 2236. Proceedings of the 18th International Conference on Radionuclide Metrology and its Applications.

Archambault, J.P., Mainegra-Hing, E., 2015. Comparison between EGSnrc, Geant4, MCNP5 and Penelope for mono-energetic electron beams. Phys. Med. Biol. 60 (13), 4951.

Basaglia, T., Han, M.C., Hoff, G., Kim, C.H., Kim, S.H., Pia, M.G., Saracco, P., 2015. Investigation of geant4 simulation of electron backscattering. http://arXiv:1506.01531arXiv:1506.01531.

Berger, M.J., 1963. Monte Carlo calculation of the penetration and diffusion of fast charged particles. Methods Comput. Phys. 2, 135–215.

Blunck, O., Leisegang, S., 1950. Zum energieverlust schneller elektronen in dünnen schichten. Z. für Phys. A Hadrons Nucl. 128 (4), 500–505.

Bobin, C., Thiam, C., Chauvenet, B., 2017. A radionuclide calibrator based on cherenkov counting for activity measurements of high-energy pure β^- -emitters. Appl. Radiat. Isot. 119, 60–65.

Bochud, F.O., Laedermann, J.-P., Sima, O., 2015. Uncertainty associated with monte carlo radiation transport in radionuclide metrology. Metrologia 52 (3), S191.

de Vismes, A., Amiot, M., 2003. Towards absolute activity measurements by ionisation chambers using the penelope monte-carlo code. Appl. Radiat. Isot. 59 (4), 267–272.

Faddegon, B.A., Asai, M., Perl, J., Ross, C., Sempau, J., Tinslay, J., Salvat, F., 2008. Benchmarking of monte carlo simulation of bremsstrahlung from thick targets at radiotherapy energies. Med. Phys. 35 (10), 4308–4317.

Galea, R., 2014. Private Commmunication. OPShowpublished, National Research Council Canada.

Goudsmit, S., Saunderson, J., 1940. Multiple scattering of electrons. Phys. Rev. 57 (1), 24.

Kawrakow, I., Bielajew, A.F., 1998. On the condensed history technique for electron transport. Nucl. Instrum. Methods 142B, 253–280.

Kawrakow, I., Mainegra-Hing, E., Rogers, D.W.O., Tessier, F., Walters, B.R.B., 2013. The EGSnrc Code System: Monte Carlo simulation of electron and photon transport. Technical Report PIRS–701 (7th printing), National Research Council of Canada, Ottawa, Canada.

Kim, S.H., Pia, M.G., Basaglia, T., Han, M.C., Hoff, G., Kim, C.H., Saracco, P., 2015. Validation test of geant4 simulation of electron backscattering. IEEE Trans. Nucl. Sci. 62 (2), 451–479.

Koch, H.W., Motz, J.W., 1959. Bremsstrahlung cross-section formulas and related data. Rev. Mod. Phys. 31 (October), 920–955.

Laedermann, J.-P., Valley, J.-F., Bulling, S., Bochud, F.O., 2004. Monte carlo calculation of the sensitivity of a commercial dose calibrator to gamma and beta radiation. Med. Phys. 31 (6), 1614–1622.

Landau, L.D., 1944. On the energy loss of fast particles by ionization. J. Phys. 8, 201–205.

Lewis, H.W., 1950. Multiple scattering in an infinite medium. Phys. Rev. 78 (June), 526–529.

Michotte, C., Pearce, A., Cox, M., Gostely, J.-J., 2006. An approach based on the SIR measurement model for determining the ionization chamber efficiency curves, and a study of 65 Zn and 201 Tl photon emission intensities. Applied Radiation and Isotopes 64 (10), 1147 – 1155, Proceedings of the 15th International Conference on Radionuclide Metrology and its Applications.

Pandola, L., Andenna, C., Caccia, B., 2015. Validation of the geant4 simulation of bremsstrahlung from thick targets below 3 MeV. Nucl. Instrum. Methods Phys. Res. Sect. B: Beam Interact. Mater. At. 350, 41–48.

Poon, E., Seuntjens, J.S., Verhaegen, F., 2005. Consistency test of the electron transport algorithm in the GEANT4 Monte Carlo code. Phys. Med. Biol. 50, 681–694.

Seltzer, S.M., 1988. Cross sections for bremsstrahlung production and electron impact ionization. Monte Carlo Transp. Electrons Photons 81–114.

Seltzer, S.M., Berger, M.J., 1985. Bremsstrahlung spectra from electron interactions with screened atomic nuclei and orbital electrons. Nucl. Instrum. Methods Phys. Res. Sect. B: Beam Interact. Mater. At. 12 (1), 95–134.

Seltzer, S.M., Berger, M.J., 1986. Bremsstrahlung energy spectra from electrons with kinetic energy 1 keV-10 GeV incident on screened nuclei and orbital electrons of neutral atoms with Z = 1100. At. Data Nucl. Data Tables 35 (3), 345–418.

Thiam, C., Bobin, C., Loureno, V., Chist, V., Amiot, M.-N., Mougeot, X., Lacour, D., Rigoulay, F., Ferreux, L., 2016. Investigation of the response variability of ionization chambers for the standard transfer of SIR-spheres. Applied Radiation and Isotopes 109, 231 – 235, Proceedings of the 20th International Conference on Radionuclide Metrology and its Applications 811 June 2015, Vienna, Austria.

Urban, L., Dec 2006. A model for multiple scattering in GEANT4. Tech. Rep. CERN-OPEN-2006-077, CERN, Geneva.

X-5 Monte Carlo Team, 2003. MCNP™ Version 5, A General Monte Carlo N-particle Transport Code. Technical report, LA-UR-03-1987, LANL.